# CHAPTER 5

# DEVELOPMENT OF NANOCELLULOSE/PROTEIN-BASED HYDROGEL THAT ENHANCES GELLING CHARACTERISTICS AND EXPOLRE ITS APPLICATIONS IN FOOD SYSTEMS

## 5.1. Introduction

Hydrogels are hydrophilic, three-dimensional networks capable of absorbing and retaining significant amounts of water or biological fluids within their structure (Abaee et al., 2017). First introduced by Wichterle and Lim in 1960, hydrogels have since found extensive applications across various fields, including food, agriculture, cosmetics, biomedicine, tissue engineering, and drug delivery. Natural-source hydrogels have garnered significant attention due to their biocompatibility and biodegradability. Among these, cellulose-based hydrogels stand out for their hydrophilicity, abundant availability, low cost, non-toxicity, and remarkable mechanical properties, making them an ideal choice for diverse applications. Structurally, hydrogels consist of crosslinked polymeric networks formed through chemical or physical interactions. These networks are typically insoluble in most physiological solvents yet possess a high capacity for water uptake (Facin et al., 2015). Their high hydration levels, combined with desirable properties such as biocompatibility, biodegradability, mechanical stability, and responsiveness, make hydrogels particularly suitable for applications in food, cosmetics, and pharmaceuticals. Notably, they are highly effective in controlled release systems for bioactive molecules (Kasai et al., 2023). These versatile characteristics highlight hydrogels as promising materials for innovative solutions across various industries.

Soy protein isolate (SPI), a plant-based protein with over 90% protein content (Petruccelli and Anon, 1995), is widely utilized in the food industry due to its low cost, abundant availability, high nutritional value, and functional properties such as solubility, emulsifying, foaming, swelling, and gelling (Guo et al., 2017; Nishinari et al., 2014). These properties make SPI suitable for various applications, including the production of tofu, processed meats (Gao et al., 2015), and as carriers for nutraceutical transport and

release (Nooshkam et al., 2020). SPI's emulsifying and gelling properties are commonly used in developing food products, particularly those mimicking or replacing fat, as SPI-polysaccharide mixtures provide a fat-like taste with lower energy content (Corredig et al., 2011). The addition of polysaccharides improves emulsion stability and modifies the aqueous medium's rheology through interactions with protein molecules (Wang et al., 2020). However, removing fat can negatively impact food texture, structure, and flavour. While SPI hydrogels exhibit high mechanical strength and ductility (Li et al., 2019), their transport efficiency as nutrient carriers in the body remains low due to rapid degradation by pepsin in the gastric environment (Yanet al., 2020).

Cellulose, a semi-rigid polysaccharide recognized as dietary fiber, is extensively used in protein-polysaccharide complexes due to its diverse physicochemical and physiological functions. These include water retention, rheological modification, emulsion stabilization, cholesterol reduction, and bowel function improvement (Schmitt & Turgeon, 2011). Derivatives like carboxymethyl cellulose (CMC) and microcrystalline cellulose (MCC) have been widely utilized. CMC serves as a fat substitute in dairy, baked goods, and low-fat meat products (Su et al., 2010). MCC, used in hamburgers and sausages, delivers physiological benefits while maintaining low fat and energy content (Gibis et al., 2015). Cellulose nanofiber (CNF), a nanoscale derivative, is nanofibrillated from lignocelluloses using high-pressure homogenizers, grinders, or ultrasonicators (Klemm et al., 2011). CNF boasts unique traits like low density, high aspect ratio, strength, biocompatibility, and biodegradability (Khalid et al., 2024), making it a promising alternative to traditional cellulose derivatives. Additionally, CNF functions as a rheological modifier due to its hydroxyl groups and high aspect ratio, enabling hydrogen bonding and gel formation at low concentrations (Rana et al., 2023). Integrating CNF into SPI significantly alters the mixtures' physicochemical properties. Factors such as pH, temperature, SPI-to-CNF ratio, total solids, and ionic strength affect the formulation process and the mixtures' dynamic and textural properties (Sun et al., 2015). Neglecting these factors may compromise product quality and consumer satisfaction.

Proteins and polysaccharides are widely used as natural hydrogel agents due to their large polymeric structures. Protein gels form through a balance of intramolecular and intermolecular forces, including hydrogen bonds, ionic bonds, disulfide bonds, and hydrophobic interactions (Puppo & Anon, 1998). However, protein gels are sensitive to

environmental factors such as ions, pH, and temperature, which can lead to flocculation, aggregation, and reduced water retention during food manufacturing and storage (Jeong et al., 2012). Polysaccharide gels, while characterized by a stiff texture, suffer from poor water-holding capacity, limited resilience, and inferior flexibility (Hou et al., 2015). To address these limitations, combining proteins and polysaccharides has emerged as an effective strategy to achieve synergistic interactions. These interactions result in complex gels with superior characteristics, including controlled phase separation and microstructural modifications. Such enhancements optimize food texture and enable the controlled release of bioactive compounds, a significant focus in food science research (Le et al., 2017; Munialo et al., 2016).

Polysaccharide-protein double-network hydrogels have emerged as a promising solution to overcome the limitations of single-network protein or polysaccharide gels while leveraging their functional properties (Yang and Yuan, 2019). These hydrogels consist of two interpenetrating polymer networks: a brittle, rigid first network that dissipates energy effectively and a ductile, flexible second network that maintains structural integrity during deformation (Tang et al., 2020; Zhao et al., 2020). Compared to protein-only hydrogels, double-network systems demonstrate superior mechanical strength and enhanced nutrient transport efficiency in the intestine. The polysaccharide network also protects proteins from degradation by pepsin and acidic conditions in the stomach, enabling effective delivery of bioactive compounds (Alavi et al., 2018). Interactions between polysaccharides and proteins create synergistic effects, diversifying gel functionality (Chen et al., 2019). Studies show that insoluble dietary fibers, such as cellulose and its derivatives, improve protein gelling properties by forming stable network structures (Zhao et al., 2019). Among these, cellulose nanocrystals (CNC) stand out due to their nanoscale effects and unique physicochemical properties. CNC incorporation not only enhances gelling properties but also balances dietary nutrients in protein gels (Gomez et al., 2016). However, limited research exists on CNC-protein composite gels and the mechanisms behind CNC-induced improvements (Xiao et al., 2020), warranting further investigation.

Frozen dairy products like ice cream are not only popular for their taste but also hold potential as vehicles for incorporating natural bioactive ingredients, thereby offering significant nutritional and health benefits. Standard ice cream products often lack nutraceutical components, creating an opportunity to enhance their health benefits through

enrichment with functional ingredients (Paul et al., 2020). β-carotene is a powerful phytochemical that can improve the nutritional profile of ice cream by introducing antioxidant properties and increasing the content of bioactive compounds, such as phenolics. However, achieving a balance between health benefits and sensory qualities remains a challenge in functional ice cream development. Ensuring that these enriched products maintain their creamy texture, pleasant flavour, and overall consumer appeal requires careful formulation and innovation. Studies suggest that incorporating β-carotene into ice cream via advanced delivery systems, such as hydrogels, could provide a solution (Mao et al., 2018). Such approaches not only preserve the sensory characteristics of the ice cream but also enhance its functional value, paving the way for healthier, nutritionally enhanced frozen desserts (Mauricio-Sandoval et al., 2023).

This study aimed to create an innovative nanocellulose/protein hydrogel with enhanced gelling properties by integrating banana rachis nanocellulose (BRNC) with soy protein isolate (SPI). The research assessed how BRNC influenced the hydrogel's water-holding capacity, gel strength, rheological behavior, and microstructural characteristics. These evaluations highlighted the synergistic interaction between BRNC and SPI, improving functional properties. Furthermore, the hydrogel's application was explored in ice cream formulations to enhance texture, stability, and nutrient bioaccessibility while reducing fat content.

## 5.2. Materials and methods

### *5.2.1. Materials*

Cellulose was extracted from freshly harvested, fully mature banana rachis (*Musa acuminata*, 'Dwarf Cavendish') obtained from local farmers in Tezpur, using the method described by Basumatary & Mahanta (2023). Soybean protein isolate (purity ≥ 99%) was purchased from Amazon, while laccase (10.8 U/mg, E.C. 3.2.1.15, derived from *Trametes versicolor*) was sourced from Sigma-Aldrich Co., India. Standard β-carotene (purity ≥ 93%) and analytical-grade chemicals were procured from TCI, SRL, and Merck.

### *5.2.2. Preparation of nanocellulose/protein-based hydrogel*

A 10% (w/v) SPI solution was prepared by dissolving SPI powder in Milli-Q ultrapure water at 25°C and stirring for 3 h. The solution was sonicated for 10 min to ensure clarity,

then stored at 4°C overnight for complete hydration. Subsequently, it underwent heat treatment at 95°C for 30 min, followed by immediate cooling to 25°C in an ice bath. The pH of the dispersion was adjusted to 7.0, maintaining a final SPI concentration of 10% (w/v). The resulting SPI stock solutions appeared as opaque straw-yellow liquids.

To prepare SPI-BRNC double network (SPI-BRNC DN) hydrogels, β-carotene-enriched BRNC stock solutions were prepared at varying concentrations and dissolved in the SPI stock dispersion. These BRNC stock solutions were gradually added to the fully hydrated SPI solution with stirring for 2 h at room temperature to ensure complete dissolution. The final BRNC concentrations in the mixed dispersions were 0.00, 0.50, 1.00, 1.50, and 2.00% (w/v). Afterwards, GDL (0.5% w/v) and laccase (0.1 U/mg) were added to the dispersions, which were immediately transferred to a 25°C water bath and incubated for 4 h to form SPI-BRNC hydrogels. The resulting hydrogels were white and opaque. As a control, an SPI hydrogel was prepared by adding only GDL to the SPI dispersion and incubating it at 25°C.

### *5.2.3. Thermal analysis*

The thermal stability of the hydrogel samples was assessed using a thermogravimetric analyser (Model TG 209 F1 Libra, Netzsch, Germany) following the method described by Xiao et al. (2020), with minor adjustments. Approximately, 3 mg of each hydrogel sample was subjected to a controlled heating process, starting from 30°C and increasing to 600°C at a consistent rate of 10°C/min. The analysis was conducted under a nitrogen atmosphere with a flow rate of 10 mL/min, ensuring an inert environment for precise thermal degradation measurements.

### *5.2.4. Texture analysis*

The textural properties of the hydrogel samples were evaluated using a Texture Analyzer (Model TAHD Plus, Stable Micro Systems, Godalming, UK). For texture profile analysis (TPA), a 30 ± 40 g sample was evenly spread on a flat surface and rolled to a uniform thickness of approximately 10 mm. Each sample underwent two consecutive compressions at a speed of 1 mm/s, with a compression depth of 20% of the sample's original height, generating a two-bite TPA curve. The interval between compressions was 75 s. The analysis evaluated key parameters such as hardness, adhesiveness, cohesiveness,

springiness, gumminess, chewiness, and resilience, offering a detailed understanding of the textural properties.

### *5.2.5. Water Holding Capacity (WHC)*

The water holding capacity (WHC) was determined using the method described by Liu et al. (2020). The hydrogels were prepared in 10 mL centrifuge tubes and centrifuged at 1,500 rpm for 10 min at 25°C using an Eppendorf 5430 R centrifuge (Germany). After centrifugation, the water was removed with a syringe, and any residual moisture was absorbed with a dry filter paper. The WHC was then calculated based on the weight of the hydrogel before and after centrifugation as follows:

$$\text{WHC } \% = \left(\frac{W_a - W_c}{W_b - W_c}\right) \times 100 \qquad \textbf{Eq. 5.1}$$

Where $\mathbf{W_b}$ is the weight of the centrifuge tube containing the gels before centrifugation, $\mathbf{W_c}$ is the weight of the empty centrifuge tube (blank), and $\mathbf{W_a}$ is the weight of the centrifuge tube with the gels after blotting off the residual water.

### *5.2.6. Dynamic rheological measurements*

Dynamic rheological properties were analysed using a rheometer (Model: Physical MCR 72, AntonPaar, Austria) equipped with a steel parallel plate (diameter: 40 mm) and a fixed gap of 1 mm (Xiao et al., 2020). Approximately 1.5 mL of the prepared solutions were subjected to a temperature sweep, starting with heating from 25 °C to 95 °C at a controlled rate of 2 °C/min, followed by cooling back to 25 °C at 5 °C/min. Measurements were conducted at a constant oscillatory frequency of 1 Hz and a strain of 1%, ensuring linear viscoelastic conditions. The storage modulus (G′), loss modulus (G″), and phase angle (tan δ) were recorded to assess the viscoelastic properties.

### *5.2.7. Application of hydrogels in ice cream*

#### *5.2.7.1. Preparation of ice cream*

Ice cream formulation and sample preparation method were adapted from Nooshkam et al. (2023) with some modifications. The formulations of ice cream are provided in **Table 5.1**. Sugar and milk powder were mixed with pre-warmed milk and cream (45°C) for 4.0 min

with a blender (Philip HR3705/10, China). The mixture was pasteurized in a water bath (LabTech) at 85°C for 10 min, and it was then cooled and stored at 4°C for 12 h to facilitate hydration of the ingredients. Then, it was homogenised using a T25 Ultra-Turrax (IKA Works, Inc., NC, USA) at 12,500 rpm for 10 min. Afterwards, vanilla was blended with the mixture for 1 min. In the next step, the hydrogel was gently added to the mixture under manual stirring, at 0, 10, 20, 30 and 40% substitution levels (cream and sugar). The mix was then transferred to a plastic container and hardened in a Chest freezer (Blue star, CHFDD300D) at -20 °C for 24 h.

**Table 5.1.** Formulations of ice cream

| **Ingredients (%, w/w)** | **Samples** | | | | |
|---|---|---|---|---|---|
| | IC-0 | IC-10 | IC-20 | IC-30 | IC-40 |
| **Sugar** | 14 | 12.6 | 11.2 | 9.8 | 8.4 |
| **Vanilla** | 0.2 | 0.2 | 0.2 | 0.2 | 0.2 |
| **Milk** | 50.8 | 50.8 | 50.8 | 50.8 | 50.8 |
| **Milk powder** | 3 | 3 | 3 | 3 | 3 |
| **Cream** | 32 | 28.8 | 25.6 | 22.4 | 19.2 |
| **DN hydrogel** | 0 | 4.6 | 9.2 | 13.8 | 18.4 |

*5.2.7.2. Colour parameters of ice cream*

The L*, a*, and b* colour indices of the ice cream stored at −20 °C was analysed using a Hunter Colorimeter (Model: Ultrascan Vis, HunterLab; Make: Reston, Virginia). The device was calibrated using a standard tile prior to the measurements. The recorded colour indices were subsequently used to calculate the ΔE values, which indicate the overall colour difference among the samples. The formula used for ΔE is as follows:

$$\text{Total colour difference } (\Delta E) = \sqrt{\Delta L^{*2} + \Delta a^{*2} + \Delta b^{*2}} \qquad \textbf{Eq. 5.2}$$

*5.2.7.3. Texture analysis of ice cream*

The hardened ice cream samples (−20 ◦C, 24 h) were subjected to a penetration test with the aid of a cylindrical probe (6-mm diameter) via a texture analyser (TA-HD-Plus, Stable Micro Systems, Godalming, UK), according to the following conditions: 25 mm penetration depth, 1.0 mm $s^{-1}$ pre-test speed, 1.0 mm $s^{-1}$ test speed, 2.0 mm $s^{-1}$ post-test speed, at room temperature. The peak force (g) was then measured and reported as the samples' hardness (Nooshkam et al., 2023).

*5.2.7.4. Overrun, gas hold-up, and melting behaviour*

The overrun of the ice cream was determined following the method described by Nooshkam et al. (2023). A measured volume of ice cream was weighed, and the overrun was calculated using **Equation 5.3**:

$$\text{Overrun (\%)} = \frac{M_1 - M_2}{M_2} \times 100 \qquad \textbf{Eq. 5.3}$$

where, $M_1$ and $M_2$ are the mass of the unit volume of the mix (g) and ice cream (g), respectively.

The gas-hold-up capacity of the ice cream was determined using a formula outlined by Nooshkam et al. (2023). This involved applying the specified equation to quantify the proportion of gas incorporated into the ice cream, which is a critical factor in assessing its texture and overall quality. The calculation procedure is detailed as follows:

$$\text{Gas-hold up (\%)} = \frac{\text{Overrun (\%)}}{\text{Overrun (\%)} + 100} \times 100 \qquad \textbf{Eq. 5.4}$$

The melting rate of ice cream was evaluated using a modified method by Zhang et al. (2018). The test was conducted at room temperature (24 ± 2°C). A 35 g ice cream sample was placed on a wire mesh, with a pre-weighed beaker positioned beneath to collect the melted portion. After 20 min at ambient temperature, the mass of the melted sample was measured, and the extent of melting was calculated using the following equation:

$$\text{Meltdown (\%)} = \frac{\text{mass of the melted sample}}{\text{mass of the sample before melt}} \times 100 \qquad \textbf{Eq. 5.5}$$

*5.2.7.5. Rheological properties of ice cream*

Rheological properties were measured using a Rheometer (Model MCR 72, Anton Paar, Austria) following the method of Yu et al. (2021). Prepared ice cream samples were placed on the rheometer plate, and the upper parallel plate (25 mm) was set to maintain a 500 μm gap. Excess liquid was absorbed using filter paper, and silicone oil sealed the slit to prevent moisture evaporation. Measurements were conducted at 4°C using a flow ramp test with a shear rate range of 0.01–100 $s^{-1}$. A frequency sweep was performed from 0.1 to 100 Hz at 4°C with a constant strain of 1.0% within the linear viscoelastic range. The storage modulus (G'), loss modulus (G"), and damping factor (tan δ) were determined using the instrument's software. Each experiment was performed in triplicate to ensure accuracy and reproducibility.

*5.2.7.6. In-vitro gastrointestinal fat digestion of ice cream*

Lipid digestion and β-carotene bioaccessibility of functional mayonnaise were assessed using a simulated *in-vitro* gastrointestinal digestion model reported by Yi et al. (2021).

Stomach phase: First, 10 mL of simulated gastric fluid (SGF) containing 3.2 mg/mL pepsin and 0.15 M NaCl was combined with 0.5 g of mayonnaise that was dissolved in 7.5 mL of ultrapure water. Next, 2.5 M HCl was added to the mixture to bring its pH down to 2.0. The mixture was then continuously stirred at 250 rpm for one hour while being incubated at 37°C in a water-jacketed beaker.

Small intestine phase: Following stomach digestion, 1M NaOH was added immediately to neutralise the liquid to pH 7.0. Then, 15 mL of simulated intestinal fluid (SIF) containing 5 mM $CaCl_2$, 20.0 mg/mL bile extract, and 1.0 mg/mL pancreatin was added. In a water-jacketed beaker, the intestinal digestion was carried out at 37°C while being continuously stirred at 250 rpm. To this, 0.1 M NaOH was administered dropwise to maintain the pH at 7.0, and the amount of NaOH added was measured over the course of a 2 h intestinal digestion simulation. Using the following formula, the amount of NaOH solution added was used to determine the degree of lipolysis (%):

$$\text{Lipolysis (\%)} = \frac{V_{NaOH} - C_{NaOH}}{2M_{lipid}} \times 100 \qquad \textbf{Eq. 5.6}$$

Where, the volume of NaOH used is denoted by $V_{NaOH}$. The concentration of NaOH applied to $C_{NaOH}$ was 0.10 M NaOH. The average molecular weight of sunflower oil (M) is indicated as $M_{lipid}$.

*5.2.7.7. β-carotene bioaccessibility*

The amount of β-carotene that was transferred from dispersed mayonnaise into micelles divided by the original amount of β-carotene in dispersed mayonnaise was used to calculate β-carotene bioaccessibility. β-carotene micelles were obtained by centrifuging the digesta after gastrointestinal digestion for 1 h with a speed of 10,000 rpm. Then, β-carotene micelles were extracted with ethanol (70%) and n-hexane (1:2, v/v) three times. The UV-vis spectrophotometer was then used to measure the amount of β-carotene at 450 nm. The bioaccessibility of β-carotene was computed using the following formula:

$$\text{Bioaccessibility (\%)} = \frac{\text{amount of } \beta\text{-carotene transferred into micelles}}{\text{amount of BC in dispersed mayonnaise}} \times 100 \qquad \textbf{Eq. 5.7}$$

### *5.2.8. Statistical analysis*

The whole experiment was conducted in triplicates and shown as means with standard deviations. One-way analysis of variance (ANOVA) in IBM SPSS 20.0 was used for statistical analysis. Duncan's multiple range test was used to evaluate significance levels at $p \leq 0.05$. The results are presented as the mean ± standard deviation from at least three independent experiments.

## 5.3. Results and discussion

### 5.3.1. Morphology of hydrogel

The visual appearance of SPI-BRNC hydrogels with varying concentrations of banana rachis nanocellulose (BRNC) and β-carotene is presented in **Fig. 5.1**. All samples appeared solid with a creamy yellow hue. As the BRNC concentration increased, the hydrogels exhibited a progressively deeper yellow colouration, attributed to the enhanced β-carotene content. Moreover, the structural integrity of the gels improved with higher BRNC content.

The apparent texture became firmer and more cohesive, reflecting the enhanced gel formation facilitated by the increased presence of BRNC. This suggests that BRNC plays a significant role in improving its structural properties, likely through its reinforcing effect and interaction with the SPI matrix.

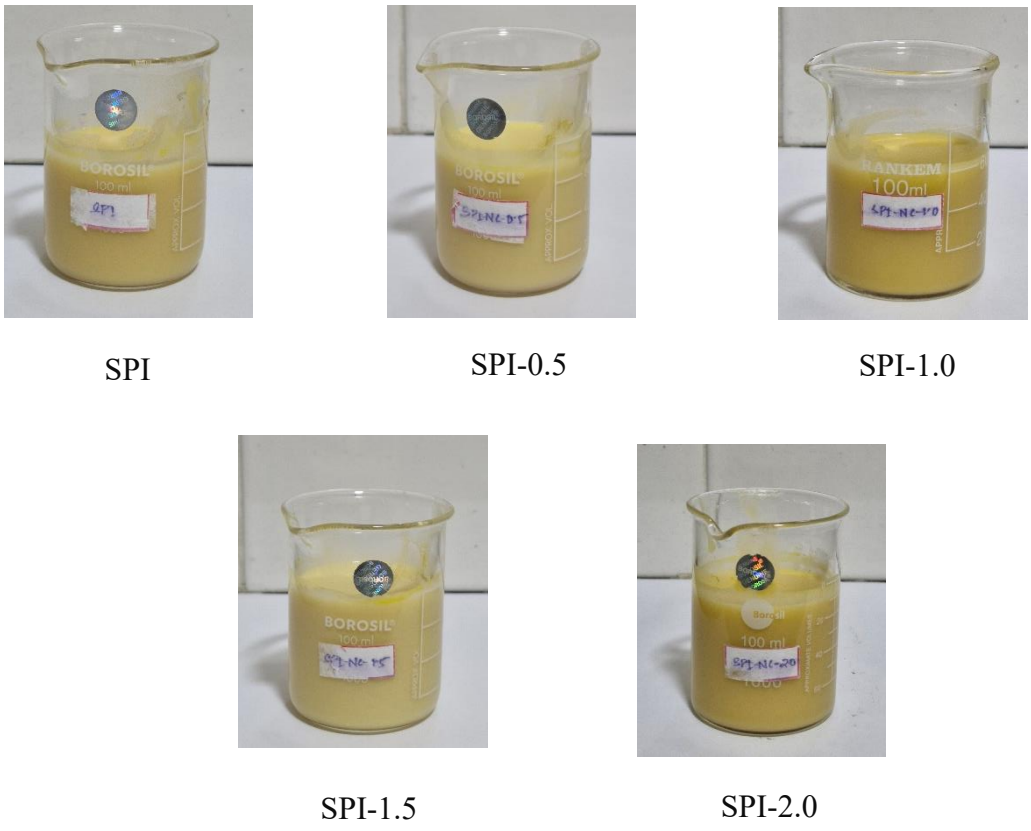


**Fig. 5.1.** Appearance of DN hydrogels loaded with different concentration of banana rachis nanocellulose (BRNC).

### 5.3.2. Thermal analysis (TGA)

**Figure 5.2** presents the TGA and derivative thermogravimetric (DTG) curves, illustrating the thermal stability of nanocellulose-reinforced hydrogels compared to pure SPI hydrogel samples. The initial mass loss observed below 100 °C is attributed to moisture evaporation, which is a typical characteristic of polymeric hydrogel systems. This weight loss corresponds to the removal of both free and bound water present in the material. Free water, often adsorbed as discrete clusters, evaporates at lower temperatures due to its weak association with the hydrogel matrix. In contrast, the desorption of structurally bound

water, which is more strongly integrated within the hydrogel network, occurs at slightly higher temperatures. These findings align with previous studies, such as Hermida-Merino et al. (2022), highlighting the distinct thermal behaviours of free versus bound water in hydrogel systems.

The temperature range of 250-350 °C showed significant mass loss, primarily attributed to the thermal degradation of protein and nanocellulose (Xiao et al., 2020). Pure SPI hydrogel exhibited a lower degradation temperature (307 °C) compared to hydrogels with nanocellulose. Notably, the incorporation of nanocellulose enhanced the thermal stability of the hydrogels in a concentration-dependent manner. Additionally, the pure SPI sample displayed a secondary degradation curve between 400 °C and 450 °C, corresponding to the decomposition of SPI (Zheng et al., 2024). These findings suggest that intermolecular interactions between SPI and nanocellulose contribute to stronger cross-linking and the formation of a stable network structure. This enhanced network improves the hydrogel's thermal stability and alters its degradation behaviour, highlighting the beneficial effects of nanocellulose addition (Xiao et al., 2020).

The DTG curves of the hydrogels revealed three distinct peaks within the temperature range of 45°–500°C. These peaks indicate improved thermal stability of the hydrogels compared to pure SPI, as evidenced by the increasing decomposition temperatures following nanocellulose crosslinking. The initial peak, around 100°C, corresponds to water evaporation, while the final peak, near 425°C, represents the degradation of pure SPI. All hydrogels also exhibited a prominent peak between 250°C and 350°C. Notably, hydrogels containing nanocellulose showed a slightly elevated degradation rate at around 320°C, underscoring the positive influence of nanocellulose on enhancing thermal stability and network integrity (Tamo et al., 2024).

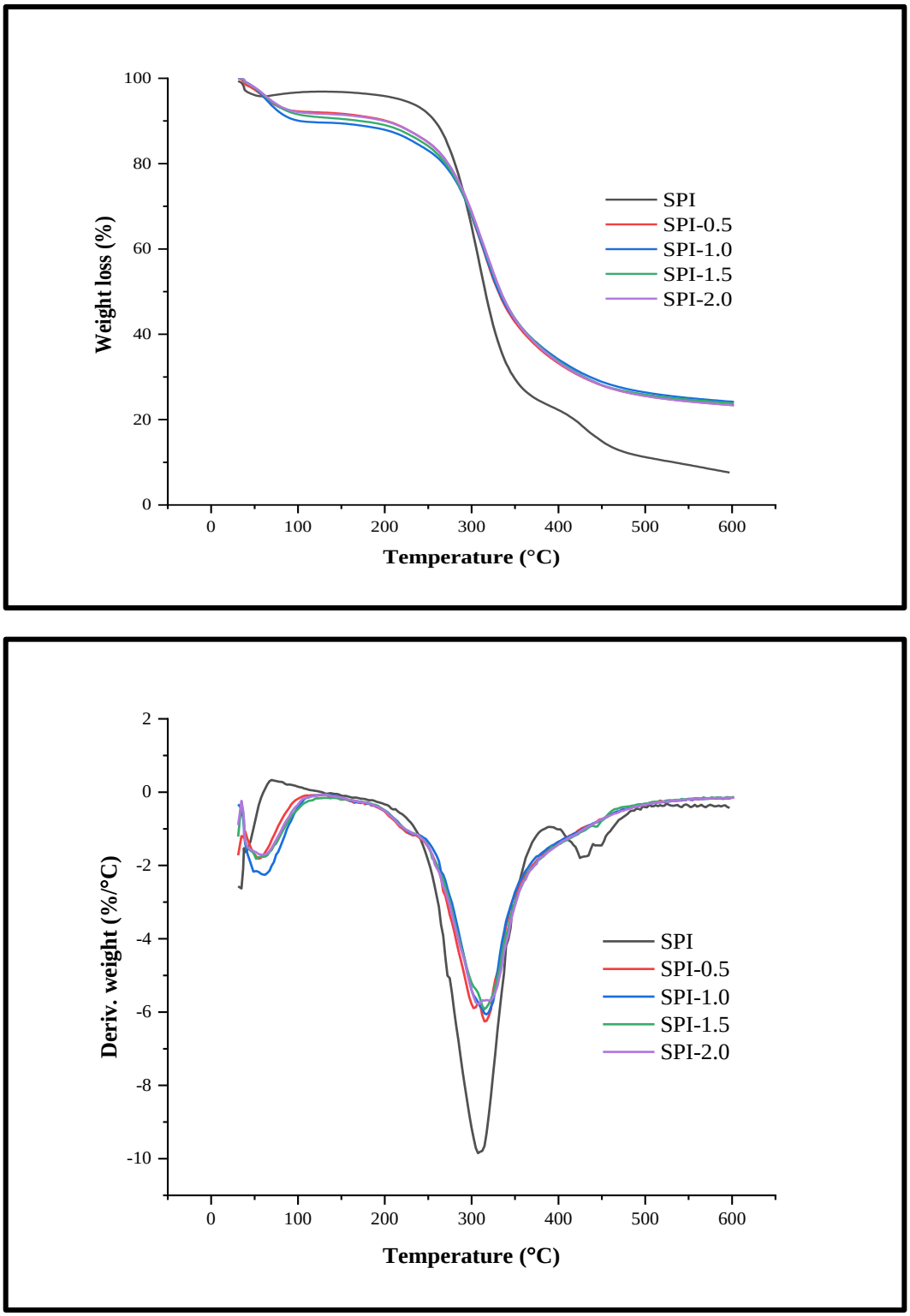


**Fig. 5.2.** Thermogravimetric analysis and 1$^{ST}$ derivatives (DTG) of DN hydrogels with different concentration of BRNC.

### 5.3.3. Texture analysis

The textural properties of hydrogel samples made from SPI, with and without nanocellulose, were analysed and compared (**Table 5.2**). TPA results showed minimal differences in springiness, cohesiveness, and resilience between the nanocellulose-enhanced hydrogels and pure SPI. Among these, springiness and cohesiveness are key parameters in TPA analysis. Springiness, which reflects the sample's elasticity, is a critical indicator of its ability to return to its original shape after compression. After the first compression, the viscoelastic properties of the sample enabled it to recover nearly to its original shape. When the interval before the second compression was sufficiently long to release internal stress, the recovery approached 100%. Cohesiveness, a parameter that reflects the material's internal bonding strength, is particularly relevant when the sample undergoes partial deformation (Chen et al., 2019). Resilience, which measures the rate of recovery after deformation, is closely associated with most TPA parameters, except for adhesiveness. The low values of springiness, cohesiveness, and resilience observed in SPI-based hydrogels are attributed to the viscous nature of SPI. In the mixture, nanocellulose acts as a stabilizer for the viscous liquid phase, enhancing the textural and structural integrity of the hydrogel. **Table 5.2** highlights the variations in hardness, gumminess, and chewiness among the hydrogel samples. Gumminess (calculated as hardness × cohesiveness) and chewiness (gumminess × springiness) are secondary parameters derived from the primary TPA values. As the concentration of nanocellulose increased, significant improvements were observed in the textural properties. Specifically, adhesiveness decreased (-8.31 to -20.04), while chewiness (25.98 to 78.82), cohesiveness (0.59 to 0.68), gumminess (36.25 to 99.29), hardness (60.78 to 145.59 g), and springiness (0.72 to 0.79) all showed marked increases, indicating enhanced structural and mechanical integrity with higher nanocellulose content. In particular, the sample with a 2% nanocellulose loading exhibited the optimal textural properties. This suggests that increasing the nanocellulose concentration enhances the gel's strength and overall texture.

Significant differences were observed in adhesiveness, which is typically assessed as the maximum tensile force developed during adhesion or as the cohesive rupture between two flat plates and the sample. Adhesiveness is closely related to hardness, as the measurement involves surface adhesiveness, hardness, and cohesiveness. Therefore, an increase in adhesive force is typically reflected by higher hardness values (Sun et al., 2015). The study

revealed an increase in hardness, gumminess, and chewiness, along with a slight decrease in adhesiveness. This reduction in adhesiveness may be attributed to the presence of nanocellulose, which acts as a filler, creating a continuous network that enhances the hydrogel's properties. With higher nanocellulose concentrations, protein molecules are more likely to cross-link with nanocellulose, increasing the formation of hydrophobic and disulfide bonds between them. This promotes a stronger gel network structure, resulting in a denser and firmer hydrogel texture (Sun & Arntfield, 2012).

**Table 5.2.** The effect of different concentration of banana rachis nanocellulose (BRNC) on texture profile of Double network (DN) hydrogel.

| **Indices** | **BRNC Concentration** | | | | |
|---|---|---|---|---|---|
| | **SPI** | **SPI-0.5** | **SPI-1.0** | **SPI-1.5** | **SPI-2.0** |
| **Hardness (g)** | 60.78 ± 0.08 | 67.32 ± 0.75 | 81.93 ± 0.42 | 127.22 ± 0.73 | 145.59 ± 0.39 |
| **Adhesiveness (g.s)** | -8.31 ± 0.56 | -11.86 ± 1.13 | -18.32 ± 0.91 | -11.34 ± 0.65 | -20.04 ± 0.11 |
| **Springiness** | 0.72 ± 0.02 | 0.75 ± 0.03 | 0.77 ± 0.02 | 0.73 ± 0.22 | 0.79 ± 0.01 |
| **Cohesiveness** | 0.59 ± 0.01 | 0.59 ± 0.02 | 0.65 ± 0.02 | 0.66 ± 0.01 | 0.68 ± 0.03 |
| **Gumminess** | 36.25 ± 0.54 | 39.67 ± 0.63 | 53.44 ± 0.42 | 84.11 ± 0.38 | 99.29 ± 1.17 |
| **Chewiness** | 25.98 ± 0.22 | 29.69 ± 1.01 | 41.01 ± 0.57 | 61.12 ± 0.25 | 78.82 ± 0.65 |
| **Resilience** | 0.17 ± 0.02 | 0.17 ± 0.01 | 0.19 ± 0.04 | 0.20 ± 0.03 | 0.20 ± 0.01 |

### 5.3.4. Water Holding Capacity

The water-holding capacity (WHC) of hydrogels is a critical indicator of their quality, as water loss can lead to gel shrinkage, texture changes, and poor-quality attributes (Liu et al., 2024). The WHC of SPI based hydrogel was 48% and increased upto 75% with the increase in BRNC concentration. In this study, the incorporation of BRNC significantly improved the WHC of SPI hydrogels, as shown in **Fig. 5.3.** Increasing the BRNC

concentration enhanced the WHC, particularly beyond 0.50%, where the composite gels exhibited significantly higher WHC than pure SPI hydrogels. This enhancement can be attributed to the improved physical entrapment of water molecules within the SPI-BRNC composite gels, resulting from the stronger intermolecular interactions in polysaccharide-protein systems (Yao et al., 2018).

The incorporation of BRNC strengthened SPI's three-dimensional network structure, contributing to its stability. The hydrophilic nature of NC, characterized by its abundant hydroxyl groups, also facilitated hydrogen bonding with water molecules, further enhancing water retention (Kasiri & Fathi, 2018). This interaction plays a pivotal role in the improved gel strength and stability of the hydrogel. The results align with previous findings that stronger intermolecular interactions and the construction of stable three-dimensional networks are essential for enhancing WHC (Liu et al., 2017; Xiao et al., 2020). Overall, the incorporation of BRNC into SPI hydrogels effectively improved WHC and gel strength by promoting hydrogen-bonding interactions and reinforcing the hydrogel's structural network. These findings underscore the potential of BRNC to develop hydrogels with desirable application properties, such as high WHC, which is crucial for maintaining gel integrity and quality during use.

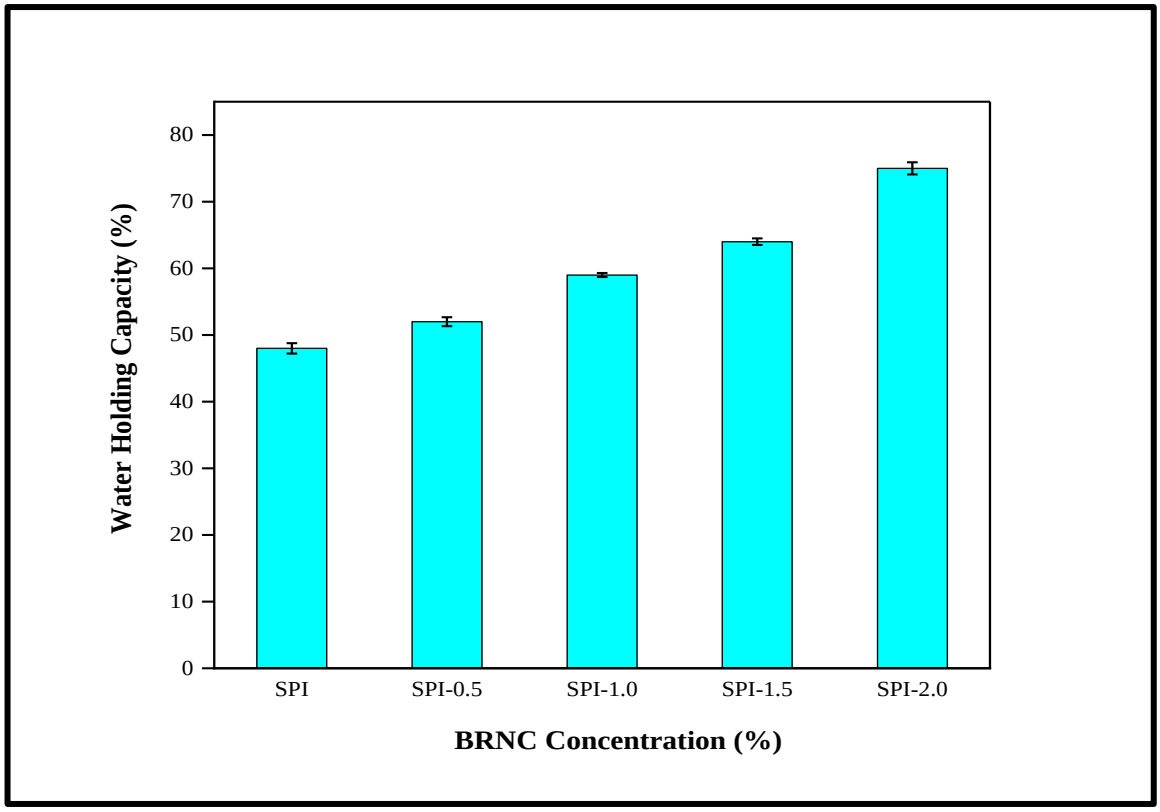


**Fig. 5.3.** Water holding capacity (WHC) of DN hydrogels with different concentration of BRNC.

### 5.3.5. Dynamic rheological properties

The viscoelastic properties of the SPI-BRNC hydrogel system were characterized by the storage modulus (G′) (**Fig. 5.4A, D**), loss modulus (G″) (**Fig. 5.4B, E**), and phase angle (tan δ) (**Fig. 5.4C, F**). The G′ values of the hydrogels were consistently higher than those of the pure SPI gel during both heating and cooling processes, with a more pronounced increase observed in hydrogels containing higher BRNC concentrations. This indicates that adding BRNC strengthens the gel structure, as G′ represents the elastic component of the material and positively correlates with gel strength (Zhou et al., 2014). These findings align with Peng et al. (2019), who observed increased firmness in whey protein isolate gels at higher bacterial cellulose microfibril concentrations. Similarly, Tomczynska-Mleko et al. (2015) reported improved rheological properties in WPI/cellulose fiber systems due to strong intra- and intermolecular interactions between protein molecules and cellulose chains. Generally, G′ ≥ 10 Pa indicates gel stability (Anderson et al., 2009). In this study, the pure SPI gel exhibited a G′ value of approximately 2000 Pa, indicating stable gelation behaviour. The BRNC network likely contributes to a modest increase in gel strength.

Importantly, the elastic modulus (G′) exceeded the viscous modulus (G″) across all samples, confirming that the SPI-BRNC system demonstrates gel-like behaviour.

The loss modulus (G″) represents the viscous component of a gel, which is directly associated with its ability to retain water, as greater viscosity correlates with improved WHC (Zhao et al., 2019). In this study, the G″ value increased progressively with higher BRNC concentrations, indicating enhanced WHC in the SPI-BRNC hydrogels. During the heating process, both G′ (elastic modulus) and G″ decreased with rising temperature, suggesting a transition from a rigid, structured state to a more fluid-like state. This reflects the thermal influence on the material's viscosity and elasticity, as reported by Xiao et al. (2020). The interactions between SPI and BRNC occur before forming a well-developed gel network. The rod-like shape of NC contributes to the system's viscosity, as their physical structure generates greater resistance, creating a more viscous composite (Xiao et al., 2020). These structural and rheological interactions underline the critical role of BRNC in enhancing the gel's functional properties.

The loss factor (tan δ), representing the ratio of viscous to elastic behaviour, provides insight into the viscoelastic properties of the hydrogels. As shown in **Fig. 5.4C, F**, the tan δ values were consistently less than 1, indicating that the elastic properties (G′) dominated over the viscous properties (G″). This confirms the gel-like behaviour of all samples, with elasticity being the predominant characteristic (Wang et al., 2018). Tan δ also serves as a descriptor of the relative viscoelastic nature of hydrogels, emphasizing their structural stability. A synergistic effect was evident in the 2.0% SPI-BRNC hydrogel group, where the G′ and G″ values were significantly higher than the combined effects of SPI and BRNC individually. This enhancement highlights BRNC's role as a rheological modifier, capable of strengthening the viscoelasticity and structural integrity of SPI hydrogels by facilitating robust intermolecular interactions.

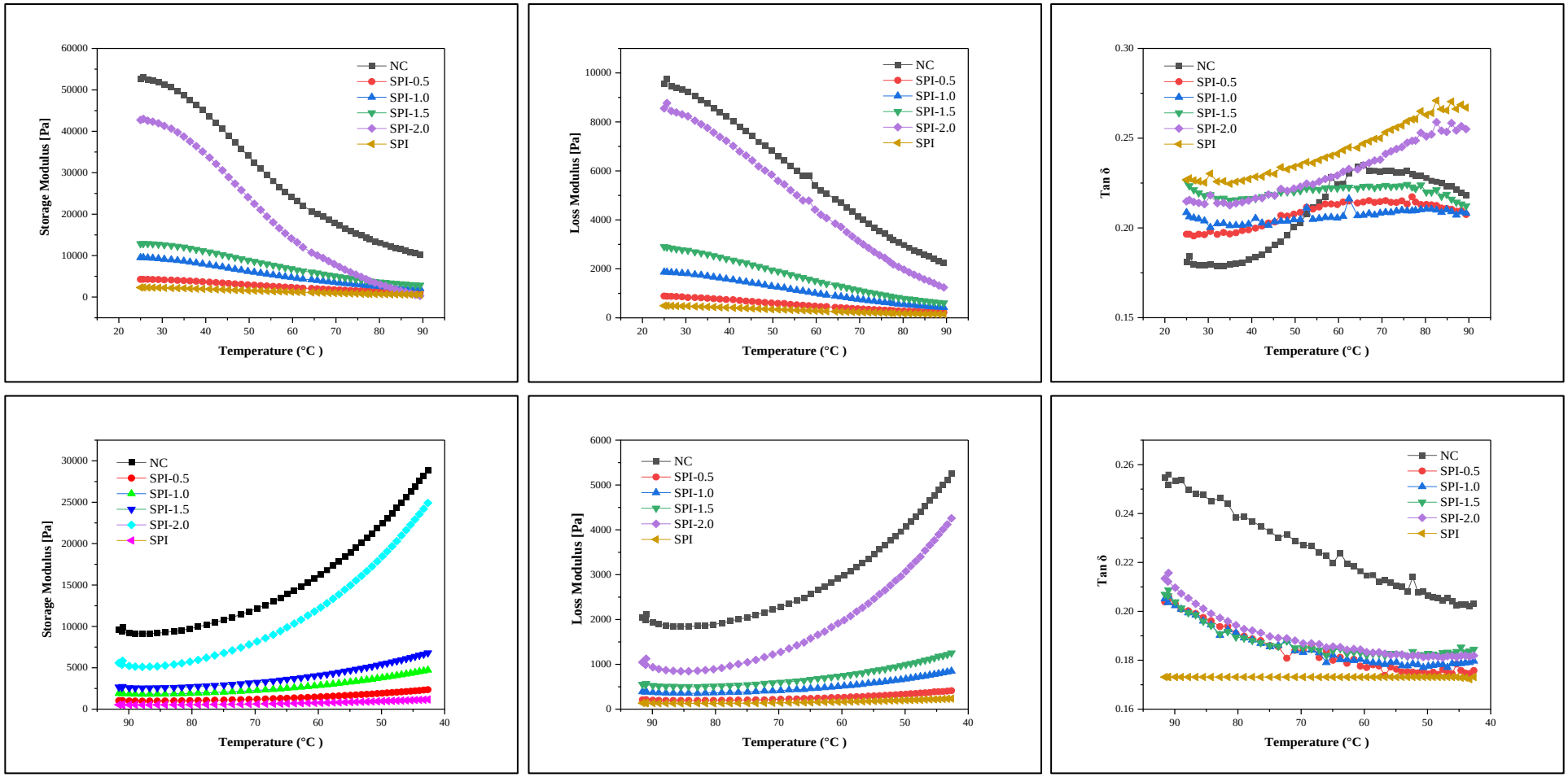


**Fig. 5.4.** Dynamic rheological properties of hydrogels at different concentration of banana rachis nanocellulose (BRNC). (A) Storage modulus G′, (B) loss modulus G″, and (C) tan δ during the heating process, (D) Storage modulus G′, (E) loss modulus G″, and (F) tan δ during the cooling process.

### 5.3.6. Application of hydrogels in ice cream

#### 5.3.6.1. Colour analysis

**Figure 5.5** displays images of ice creams prepared using β-carotene-enriched hydrogels, highlighting their texture and colour variations with increasing hydrogel incorporation. The hydrogels contributed to maintaining a smooth texture while enhancing the ice cream's visual appeal through gradual colour intensification. Table 5.3 provides detailed colorimetric data of the prepared ice creams. The results demonstrated that the addition of β-carotene-enriched hydrogels significantly influenced the colour properties of the ice cream. Incorporating these hydrogels into the ice cream mix led to a notable decrease in lightness (L*), accompanied by increases in redness (a*) and yellowness (b*), reflecting a visible shift in colour intensity. Specifically, the lightness value dropped from 35.10±0.73 to 27.80±0.12, while redness increased from 5.52±0.08 to 6.98±0.08, and yellowness rose from 9.11±0.05 to 10.61±0.29 as the hydrogel concentration increased from 4.6% to 18.4%. These changes highlight the impact of β-carotene in enhancing the ice cream's colour vibrancy and richness.


**Fig. 5.5.** Images of ice creams incorporated with β-carotene-enriched hydrogels.

The ΔE values, representing the overall colour difference among samples, were used to assess the visual impact of β-carotene-enriched hydrogels in ice cream. These values indicate the extent of colour variation between the hydrogel-enriched samples and the control (IC-0) ice cream. The results, detailed in Table 5.3, showed that the lowest ΔE value was observed for the IC-10 sample (~3.62), while the highest was recorded for the IC-40 sample (~11.18), with both differences statistically significant ($p < 0.05$). According to prior research, a ΔE value of at least 3.7 is required for the human eye to discern colour differences (Guo et al., 2018; Nooshkam et al., 2023). Therefore, the IC-10 sample's colour difference from the control was negligible, indicating a lack of perceptible variation. In contrast, IC-20, IC-30, and IC-40 samples exhibited significantly higher ΔE values, confirming noticeable colour differences compared to the control, attributable to the increased hydrogel concentration.

**Table 5.3.** Colour parameters of ice cream

| Sample | L* | a* | b* | ΔE |
|---|---|---|---|---|
| **IC-0** | $38.39\pm0.49^{a}$ | $4.16\pm0.22^{e}$ | $8.43\pm0.16^{d}$ | – |
| **IC-10** | $35.10\pm0.73^{b}$ | $5.52\pm0.08^{d}$ | $9.11\pm0.05^{c}$ | $3.62\pm0.81^{d}$ |
| **IC-20** | $32.53\pm0.35^{c}$ | $5.94\pm0.09^{c}$ | $9.58\pm0.03^{b}$ | $6.23\pm0.57^{c}$ |
| **IC-30** | $29.76\pm0.96^{d}$ | $6.19\pm0.17^{b}$ | $9.72\pm0.32^{b}$ | $8.96\pm1.04^{b}$ |
| **IC-40** | $27.80\pm0.12^{e}$ | $6.98\pm0.08^{a}$ | $10.61\pm0.29^{a}$ | $11.18\pm0.49^{a}$ |

Different letters indicate significant differences between samples at $p < 0.05$.

### 5.3.6.2. Texture analysis

The textural properties of ice cream, including hardness, cohesiveness, gumminess, adhesiveness, and chewiness were evaluated (Table 5.4). The addition of hydrogels significantly influenced these textural attributes. Notably, hardness, gumminess, and chewiness increased, while adhesiveness decreased, and only slight variations were observed in cohesiveness. Specifically, the hardness increased from 2197.42 g to 7316.82 g, cohesiveness from 0.07 to 0.09, gumminess from 147.23 to 651.19, and chewiness from 49.29 to 165.88, with adhesiveness decreasing from -62.68 to -189.09 g.s with an increase in hydrogel concentration from 0% to 40%.

The hardness of ice cream is influenced by several factors, including the viscosity of the ice cream mix, air content, solid content, ice crystal size, and ice phase volume (Muse & Hartel, 2004; Yan et al., 2022). Enhanced viscosity has been shown to increase resistance to penetration, leading to higher hardness values (Muse & Hartel, 2004). Air bubbles in the system can also act as active filler particles, with their close packing and connections contributing to increased strength (Nooshkam et al., 2023). Medium-fat ice cream has been reported to exhibit three times the hardness of high-fat samples (Guinard et al., 1996). The incorporation of hydrogels into ice cream further enhances hardness. This effect may result from the strong binding of hydroxyl groups to form a stable structure through hydrogen bonding. Moreover, hardness is influenced by fat content. Higher fat levels inhibit the formation of large ice crystals because fat globules embed in tiny ice crystals, resulting in smoother and softer ice cream (Yu et al., 2020). Conversely, reducing fat content can increase hardness due to the compensation of fat with water, which promotes the formation of larger ice crystals (Pintor et al., 2017). These larger ice crystals, along with the structural reinforcement provided by hydrogels, contribute to the overall increase in hardness.

The replacement of fats with hydrogels further enhanced the firmness of the ice cream compared to samples without hydrogel addition. This increase in firmness can be attributed to the water-holding capacity of SPI-BRNC hydrogels. As previously reported by Xiao et al. (2020), soy protein isolates and cellulose-hydrogels can bind water molecules and form a particle gel network, thereby improving the product's firmness. This effect has also been highlighted by Xiao et al. (2021).

**Table 5.4.** Texture parameters of ice cream

| Samples | Hardness (g) | Cohesiveness | Gumminess | Adhesiveness (g.s) | Chewiness |
|---|---|---|---|---|---|
| IC-0 | 2197.42 | 0.07 | 147.23 | -62.68 | 49.29 |
| IC-10 | 3003.92 | 0.05 | 162.21 | -74.89 | 71.38 |
| IC-20 | 3536.04 | 0.06 | 224.47 | -101.23 | 102.97 |
| IC-30 | 5627.45 | 0.07 | 405.18 | -155.85 | 104.61 |
| IC-40 | 7316.82 | 0.09 | 651.19 | -189.09 | 165.88 |

### 5.3.6.3. Overrun, gas hold up, and melting behaviour

**Figure 5.7** illustrates the effect of hydrogel addition on the overrun of bioactive-enriched ice cream, which reflects the amount of air incorporated during manufacturing. Overrun is a critical parameter, influencing the texture, stability, and sensory properties of ice cream during frozen storage. It is defined as the increase in volume and decrease in weight due to air incorporation and is expressed as a percentage. Incorporating hydrogel with nanocellulose and β-carotene significantly enhanced overrun. The increase in hydrogel concentration led to a proportional rise in overrun, with values of 47%, 50%, 60%, and 67% observed for ice cream substituted with 10%, 20%, 30%, and 40% hydrogel per 100 g, respectively. Air bubbles play a key role in enhancing viscosity, firmness, and stability while reducing the melting rate. This effect is attributed to the poor heat conductivity of air and improved fat destabilization during freezing (Sofjan & Hartel, 2004). The overrun of the IC-40 sample (67%) was higher than that of IC-10 and the control (38%) and approached the optimal value of 70% suggested by Flores & Goff (1999) to prevent ice crystal collisions. These findings align with studies by Mohammed et al. (2020), indicating improved stability of the ice cream mix. However, the observed overruns were lower than those reported by Borrin et al. (2018), who achieved overruns of 129–144% in curcumin-nanoemulsion ice cream. Furthermore, hydrogel addition enhanced overrun rates while decreasing the melting rate, leading to a superior product. Similar improvements were observed by Balthazar et al. (2015) and Xavier & Ramana (2022), who reported enhanced overrun, texture, and sensory scores in ice cream supplemented with 1.0%–3.0% galacto-oligosaccharides. Thus, hydrogel addition offers a promising approach to improve the functional and sensory attributes of ice cream.

The gas-hold up (or porosity) of the samples exhibited a similar trend to overrun, with the highest and lowest levels observed in the IC-40 sample (40%) and IC-0 control (23%), respectively. This improvement in gas-hold up can be attributed to the higher viscosity of hydrogel-loaded mixes, even at reduced solid content such as sugar and fat. The increased viscosity likely facilitated the incorporation and stabilization of air pockets, enhancing the aeration of the ice cream mixture. Additionally, the foam used in these formulations contained SPI and BRNC, both known for their excellent overrun capacities, as extensively documented in previous studies (Nooshkam et al., 2023). These components likely

contributed to the improved aeration properties, ensuring the formation of stable air bubbles and enhancing the overall texture and quality of the ice cream.

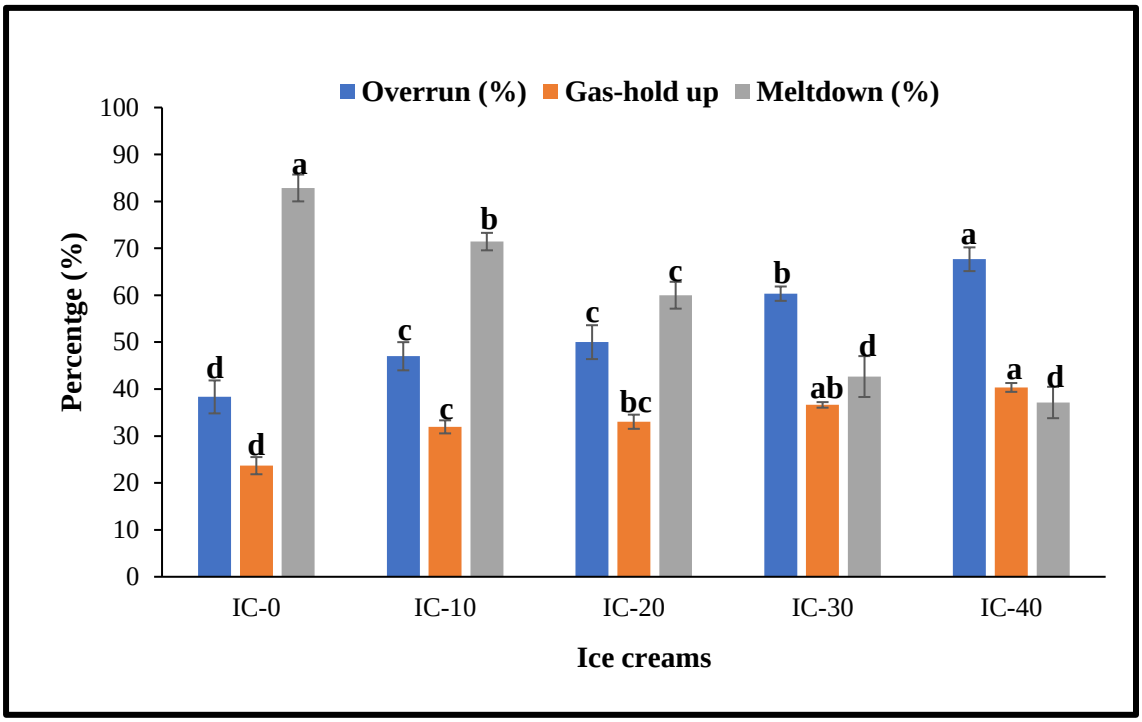


**Fig. 5.6.** Overrun, gas-hold up, and meltdown of ice creams. Different letters indicate significant differences between samples at $p < 0.05$.

**Figure 5.6** illustrates the melting rates of hydrogel-based ice cream samples, which decreased significantly with increased hydrogel concentration. The melting rate for ice cream containing 10% hydrogel per 100 g was 71.43%, decreasing to 60%, 42.67%, and 37.14% for 20%, 30%, and 40% hydrogel, respectively. This trend indicates that higher hydrogel concentrations substantially reduce the melting rate. The reduced melting rate can be attributed to higher overrun, as ice creams with greater air content melt more slowly due to reduced thermal diffusivity, minimizing heat penetration into the product (Sofjan & Hartel, 2004). Additionally, Xavier and Ramana (2022) noted that higher cellulose fiber concentrations prolong melting times, while Feizi et al. (2021) demonstrated that stabilizers such as basil seed gum enhance viscosity, thereby increasing melting resistance.

Melting properties are influenced by overrun, serum phase viscosity, and fat destabilization (Wu et al., 2019). In this study, the meltdown levels ranged from 82.86% in the control sample (IC-0) to 37.14% in IC-40, with hydrogel-loaded samples showing significantly lower meltdown than the control ($p < 0.05$). An inverse relationship between

overrun and melting rate was observed, as higher overrun slowed melting. Air cells function as insulators, reducing thermal diffusion and delaying the meltdown process (VanWee et al., 2020). This explains the superior thermal resistance of hydrogel-containing samples with higher overrun and gas-hold up, emphasizing the thermal benefits of hydrogel incorporation.

#### 5.3.6.4. Rheological properties

**Figure 5.7** illustrates the rheological behaviour of ice cream mixes, showing shear stress versus shear rate (**Fig. 5.7A**) and viscosity versus shear rate (**Fig. 5.7B**). The ice cream mixes exhibited non-Newtonian, shear-thinning characteristics, where viscosity decreased as shear rate increased, confirming pseudoplastic behaviour. This aligns with the findings of Goff and Davidson (1992), who reported similar flow behaviour in ice cream mixes. The IC-0 sample had the highest viscosity, while IC-40 showed the lowest, demonstrating the impact of hydrogel concentration. The decrease in viscosity with increasing shear rate is attributed to interactions among the complex components of ice cream, such as fat, proteins, sugars, and hydrogel. These interactions result in a reduction in viscosity under shear forces, contributing to the creamy texture of ice cream. Hydrogel addition balanced the shear-thinning behaviour of the samples, a phenomenon consistent with observations by Kaya and Tekin (2001) in ice cream mixes with varying salep content. The shear-thinning behaviour is partly related to fat globule aggregation, where shearing reduces fat globule size, affecting mix viscosity (Yu et al., 2020). Viscosity significantly influences overrun, as higher viscosities enhance air incorporation during freezing, promoting smaller air cell formation and higher overrun values (VanWees et al., 2020; Warrenet al., 2018). However, excessive viscosity may reduce whipping efficiency, making a balance essential for optimal air retention and texture (Feizi et al., 2021). Thus, viscosity is a critical factor in achieving the desired rheological and sensory properties in ice cream.

A frequency sweep test was conducted to assess the viscoelastic behaviour of ice cream samples, as depicted in **Fig. 5.7 (C–E).** The elastic modulus (G') and viscous modulus (G") increased with frequency across all samples. The test revealed that the addition of hydrogel to ice cream enhanced its viscoelastic properties by increasing both G' and G". However, the G' and G" values decreased with higher hydrogel concentrations, and this effect was more pronounced in IC-30 and IC-40 samples compared to the control (IC-0). Typically, a higher G' corresponds to a firmer, more rigid texture. This was evident in the

control sample (IC-0), which exhibited the highest G' value, indicating a solid-like elastic structure. In contrast, hydrogel-containing samples, particularly IC-30 and IC-40, had reduced G' values due to the presence of nanocellulose, leading to a softer texture. **Fig. 5.7D** highlights the higher G" values in hydrogel-containing samples, which indicate more liquid-like behaviour. This softer, more fluid texture contributes to a creamier and smoother mouthfeel. Additionally, a higher G" is often associated with faster melting rates, as the structure is less rigid and more prone to flow. This liquid-like property also correlates with higher overrun, giving the ice cream a lighter, airier texture.

The loss factor (tan δ), representing the ratio of viscous to elastic properties, is shown in **Fig. 5.7E.** Materials with tan $\delta < 1$ exhibit predominantly elastic behaviour, while those with tan $\delta > 1$ are more viscous (Nooshkam et al., 2022). The results indicated varied textural characteristics among the samples. IC-10 and IC-20 showed tan δ values less than 1, demonstrating the dominance of elastic (solid-like) properties. On the other hand, IC-0 and IC-30 exhibited tan δ values greater than 1, indicating the prevalence of viscous (liquid-like) behaviour. Interestingly, IC-40 had a tan δ value of approximately 1, signifying a balanced viscoelastic property. This balance in IC-40 creates a texture that is neither too firm nor too soft, combining the advantages of both elastic and viscous properties. These findings suggest that hydrogel incorporation can significantly influence the structural and textural characteristics of ice cream, allowing for the customization of its sensory qualities.

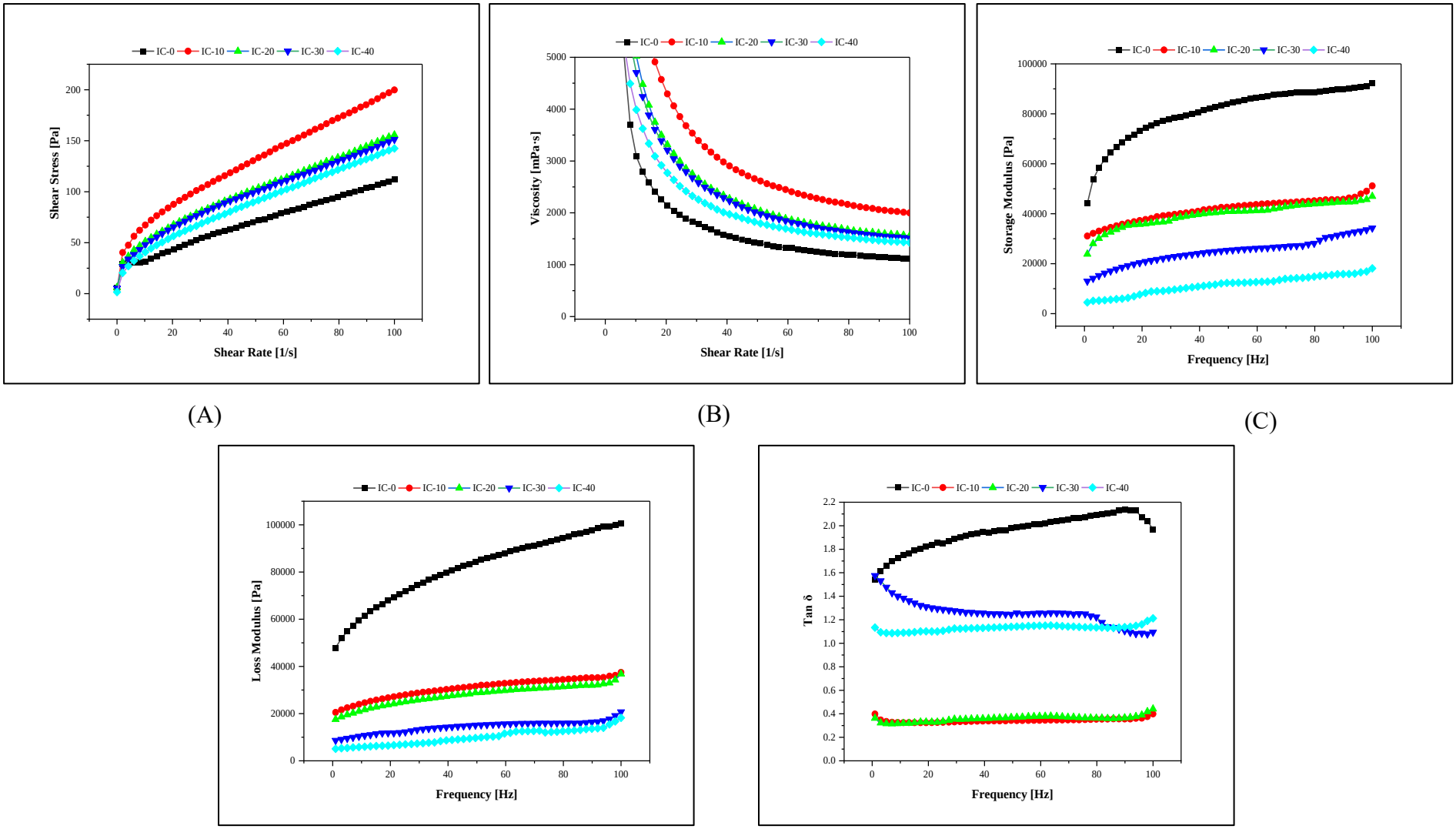


**Fig. 5.7.** (A) Shear stress, (B) Apparent viscosity, (C) Storage modulus (G'), (D) Loss modulus (G"), and (E) Tan δ of ice creams.

### 5.3.6.5. *In vitro* gastrointestinal fat digestion of ice creams

**Figure 5.8** illustrates the percentage of free fatty acids (FFA) released from SPI-BRNC-loaded hydrogel samples during two hours of digestion. A sharp increase in FFA release occurred within the first 10 min, followed by a slower rise. The control sample exhibited a higher initial rate and overall extent of lipid digestion compared to the hydrogel-added samples. This difference is likely due to variations in fat droplet organization. In the control, unstable fat droplets aggregated under simulated gastric conditions but dispersed in the intestinal phase as the gel matrix disintegrated, exposing a large lipid surface area to lipase and promoting rapid digestion. Conversely, the SPI-BRNC-loaded hydrogel samples displayed stable fat droplets under gastric conditions, but these droplets aggregated in the intestinal phase, reducing the lipid surface area accessible to lipase and slowing digestion. This phenomenon aligns with findings by Mun et al. (2015), which emphasize the influence of matrix structure on lipid digestion dynamics.

As hydrogel concentration increased, the initial release rate and total FFA release decreased, suggesting that higher hydrogel concentrations create a barrier that delays hydrolysis and reduces the effectiveness of bile salts and lipases in promoting lipolysis. After one hour of digestion, the release of FFAs exhibited a slight and gradual decrease in comparison to control with higher hydrogel concentration. This effect might be explained by the hydrogel replacing part of the fat, reducing the hydrolysed total fatty acid content, and inhibiting fat digestion in ice cream. These results are consistent with findings from previous studies. For instance, Deloid et al. (2018) reported that adding nanocellulose to high-fat food reduced fat digestion by decreasing triglyceride hydrolysis due to fat droplet coalescence on fibrillar NC (CNF) fibers, which reduced the surface area available for lipase binding. Similarly, Liu, Kerr, and Kong (2019) demonstrated that adding 0.30% (w/w) CNF to milk fat reduced FFA release during intestinal digestion by promoting lipid droplet coalescence and inhibiting fat hydrolysis. Based on these findings, it can be concluded that the presence of nanocellulose and SPI in hydrogels not only reduces fat content in ice cream but also has an inhibitory effect on fat digestibility in the human intestine. However, the low initial fat content resulted in lower FFA release during simulated intestinal digestion. Therefore, further investigation is required to evaluate ice cream samples with the same fat content, with and without hydrogel addition.

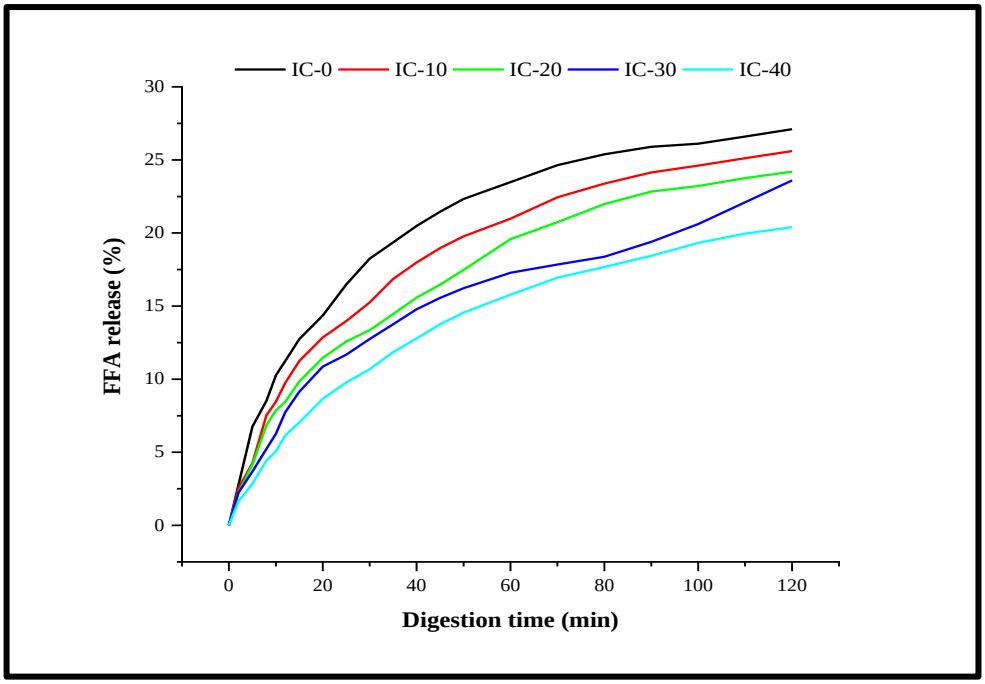


**Fig. 5.8.** Free fatty acids release during digestion of ice cream.

### 5.3.6.6. β-Carotene bioaccessibility

β-carotene is susceptible to chemical degradation when exposed to external conditions, such as light, oxygen, temperature, and free radicals (Liu et al., 2018). To solve this problem, SPI-BRNC-loaded hydrogel systems was developed and added to the ice cream in order to provide protection against such external conditions as well as to increase the stability of β-carotene in food system (Silva et al., 2021). **Figure 5.9** shows the β-carotene bioaccessibility of ice cream samples after in-vitro digestion. The bioaccessibility of β-carotene increased from 12% to 19% with the addition of hydrogel to ice cream. The stability of a substance like β-carotene during digestion and its subsequent absorption by the body determines its health benefits. To ensure that β-carotene can be efficiently absorbed and provide health advantages, it is crucial to examine the impact of the hydrogel system on its stability and absorbability during in-vitro digestion.

The bioaccessibility of β-carotene was significantly higher in IC-40 (19.8%) compared to IC-10 (12.3%), likely due to the differences in hydrogel concentration between the two samples. In IC-40, the higher concentration of cellulose nanoparticles forms a more stable interfacial film around the oil droplets, creating a protective barrier that prevents extensive oxidation or degradation of β-carotene in harsh gastric and intestinal environments. This

stability enables more β-carotene to be released and absorbed, improving its bioaccessibility (Yi et al., 2021). Conversely, IC-10, with a lower hydrogel concentration, provides less protection to β-carotene, resulting in reduced bioaccessibility. Additionally, the IC-40 sample may shield β-carotene from deterioration in the acidic stomach environment, indicating improved chemical stability. The structure of IC-40 better preserves β-carotene integrity during digestion compared to IC-10, contributing to higher bioaccessibility despite reduced lipolysis rates. This enhanced retention of β-carotene within the IC-40 structures leads to increased bioavailability after digestion (Qi et al., 2020). These findings highlight the critical role of hydrogel stability and structure in enhancing the bioavailability of β-carotene during digestion.

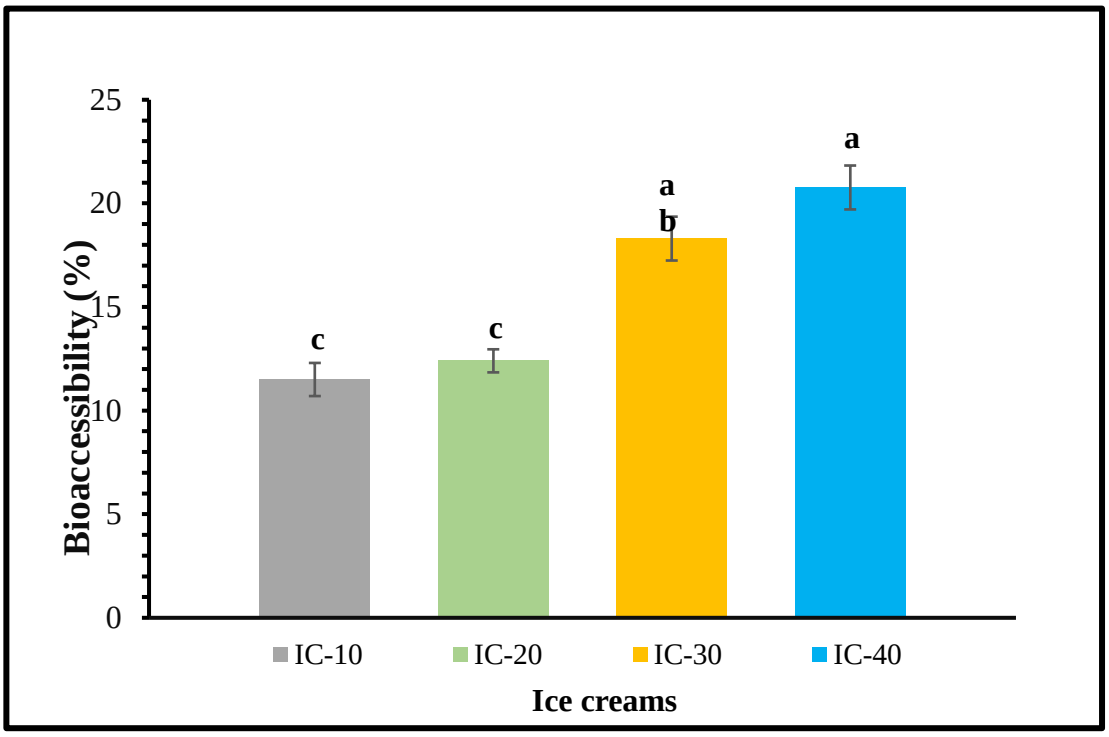


**Fig. 5.9.** Bioaccessibility of β-carotene in ice creams.

## 5.4. Conclusion

The incorporation of BRNC into SPI-based hydrogels and ice cream formulations demonstrated significant enhancement in functional, structural, and nutritional properties. Increasing the BRNC concentration from 0.5% to 2% (w/v) improved the water-holding capacity, gel strength, thermal stability, and viscoelasticity of the SPI hydrogel, making it more robust and suitable for diverse applications. Colour analysis revealed that higher hydrogel content reduced lightness (L*) while increasing greenness (a*) and yellowness (b*). These changes in appearance were accompanied by functional benefits, such as increased overrun and gas-hold up in ice cream, along with a reduction in melting rate. These attributes contribute to a stable, airy structure and slower melting, enhancing the sensory experience. Texture profile analysis showed a significant increase in hardness, gumminess, and chewiness with higher hydrogel concentrations, highlighting its ability to improve the structural integrity of ice cream. Rheological studies confirmed that ice cream mixes exhibited non-Newtonian, shear-thinning behaviour, where viscosity decreased with increasing shear rate. This behaviour enhanced the creamy texture of the ice cream, with IC-40 achieving an optimal balance between creaminess and texture, making it the preferred formulation. The inclusion of hydrogel also introduced nutritional benefits, notably reducing fat content by up to 20.4% in IC-40. This reduction was achieved without compromising texture or stability, suggesting its potential in developing lower-fat ice cream formulations. Furthermore, in vitro digestion studies revealed that the hydrogel inhibited fat digestibility, primarily due to the coalescence of fat droplets, which can contribute to a healthier lipid profile in the diet. In addition, the hydrogel enhanced the bioaccessibility of β-carotene, a key nutrient, increasing its availability from 12.3% in IC-10 to 19.8% in IC-40 within the small intestine. This improvement underscores the hydrogel's role in delivering enhanced nutritional value. Overall, BRNC hydrogel is a multifunctional ingredient that improves the structural, sensory, and nutritional properties of ice cream, offering a promising solution for developing healthier and higher-quality frozen desserts. These findings contribute to the innovative use of nanocellulose/protein-based hydrogels in creating healthier, high-quality frozen desserts.